International Journal Of Advances In
ENGINEERING, SCIENCE, COMMERCE, MANAGEMENT AND LAW
(IJAESCML)

ISSN (Online)
3048-8427
Vol. 3 | Issue 3
2026

www.ijaescml.com | internationaljournal1234@gmail.com | Peer Reviewed & Refereed Journal

[Behaviour of Long-Span Steel Truss Systems with Different Geometrical Configurations under Lateral Loads Using STAAD.Pro]

Ritambhara Ladiya*[1], Dr. Rahul Kumar Satbhaiya*[2]

*[1] MTech Scholar, Civil Department, Infinity Management & Engineering College, Sagar

*[2]Guide and HOD, Civil Department, Infinity Management & Engineering College, Sagar

ABSTRACT

Long span steel roof structures are widely used for industrial shed, warehouse, hangar, exhibition hall and other buildings which require that the space between columns is unobstructed. Of all the structures forms available, the triangulated truss is the most material efficient method of spanning large distances as the members are idealised to work under axial tension or compression. The internal geometry of a truss roof is, however, very critical to its lateral-load performance, as is the cross sectional shape of the members. With the three most popular long span roof truss designs, namely, the Fink (Flink), Howe and the King Post, and three typical steel sections provided as specified in Indian Standards, namely, Indian Standard Medium Weight Beams, rolled steel channel and rolled steel angle, there are a total of nine structural categories under examination in this paper. A typical eave height of 3.5 m for the representative industrial building of 35 m × 25 m plan was modelled and analysed in the STAAD software.Pro for combined dead, live and lateral wind loading as per IS 875 (Part 3):2015 for basic wind speed of 39 m/s. 15 independent and combined load cases were analyzed and the shear force, axial force, support reaction and nodal deflection were then extracted and compared systematically for each configuration. The results demonstrate that the Howe truss configuration always has the lowest peak shear force, axial force, support reaction, and deflection as compared with the other two types of trusses (Fink and King Post); and that the ISMB (beam) section has the lowest peak force in all the variables as compared to the other two sections (channel and angle). A comparison of the costs based on quantity further suggests that the Howe truss built of ISMB sections is the most economic of the nine configurations studied, and is therefore recommended as the best configuration for long span industrial roofs of the size investigated.

KEYWORDS: Long-span steel structures, Roof truss geometry, Howe truss, Fink truss, King Post truss, Lateral wind load, STAAD.Pro.

Received	Accepted	Published	Article Type
15/05/2026	27/07/2026	31/07/2026	Research Paper

International Journal Of Advances In
ENGINEERING, SCIENCE, COMMERCE, MANAGEMENT AND LAW
(IJAESCML)

ISSN (Online)
3048-8427
Vol. 3 | Issue 3
2026

www.ijaescml.com | internationaljournal1234@gmail.com | Peer Reviewed & Refereed Journal

1. Introduction

For a variety of applications, including manufacturing, warehousing, aircraft maintenance and indoor sporting events, industrial and commercial construction has been increasingly requiring large, column-free floor areas. In general, for spans between 20 to 25 m, the self-weight of the steel girders required to control flexural stress and deflection increases disproportionately to the span length, leading to structural inefficiency.Reinforced concrete or solid-web steel girders become structurally inefficient when the span is greater than about 20–25 m, because the self-weight of the girders needed to control flexural stress and deflection increases disproportionately with span length. An alternative material solution is the triangulated steel truss: by breaking down the roof structure into a pin-jointed framework of members, each element is idealised to be subjected to either tensile or compressive forces only, and spans of over 30 m can be achieved with relatively small amounts of steel.

However, there are two interrelated design decisions that significantly affect the structural performance of a truss roof: the geometric pattern of the arrangement of the top chord, bottom chord and web members and the cross-sectional shape that is given to each member. In practice several different truss configurations are developed, such as the Pratt, Warren, K-truss, Howe, Fink and King Post, which are different in terms of the direction and frequency of web members, and hence in the way that the axial force is transmitted from the load to the supporting structure. In Indian industrial practice rolled steel angles, channels and Indian Standard Medium Weight Beam (ISMB) are the most commonly specified in truss members, because they are readily available and have well defined design provisions in IS 800:2007.

Long-span truss roofs in cyclone prone or high wind areas must be designed to resist significant lateral wind loads, most commonly the size of members and lateral stability of the roof. IS 875 (Part 3):2015 is an updated version of the earlier code of 1987, which introduces changes to design wind pressure calculation factors for terrain roughness, topography and risk co-efficient that may result in significant differences when comparing studies conducted before and after the change.

Structural analysis and design software that can be integrated is available.Pro has vastly simplified the comparative study of the different truss configurations and sections, and can model, analyse and post process multiple truss configurations in a consistent and same computational environment. Although there are many previous studies that have investigated both geometry and section size optimisation of a truss, as reviewed in Section 2, there are relatively few studies that examine the optimisation of the truss geometry and the member sections at the same time in a single, consistently modelled parametric study, let alone simultaneously compare the truss structure with a quantity-based cost analysis.

This paper aims to fill that void by conducting a comparative study of the nine configurations of the Fink, Howe and King Post truss geometries, all of which are modelled with angle, channel and ISMB sections, for a representative long span (35 m x 25 m) industrial building under combined dead, live and lateral wind load as specified in IS 875 (Part 3):2015. The literature review is presented in Section 2 and the specific research gap is identified in Section 3, while the objectives of the study are presented in Section 4, and the methodology used, namely geometry, loading and STAAD, are described in Section 5.Pro modelling procedure adopted; (Section 6 shows results and discussion, and (Section 7 and 8 show the graphical and tabular comparisons respectively), (Section 9 shows the comparison of structure and economy), (Section 10 concludes the paper and gives some directions for future work).

2. Literature Review

Research relevant to the structural behaviour under wind loads of steel trusses can be summarised under four headings: refinement of the wind-loading procedures in codes; monitoring of the behaviour of long-span truss structures in service; metaheuristic and machine-learning-based optimisation of truss sizing and topology; and a large number of foundational comparative studies that established truss geometry and member section as the key design variables.

Suthar and Goyal [1] have compared the results of storey shear and lateral deflection calculated based on superseded IS 875 (Part 3):1987 and current IS 875 (Part 3):2015 wind provisions in STAAD.Pro reported that the revised code leads to a 15.6–

ISSN (Online)
3048-8427
Vol. 3 | Issue 3
2026

25.9% decrease in computed wind force depending on direction, a result that has implications for the wind loading assumptions used in the present study. In-plane and fatigue tests are respectively conducted by Zhang et al. [2] and Liu et al. [3] to study the in-plane and fatigue behaviour of long-span truss-based floor and bridge-deck systems under lateral loading and cyclic loading, respectively, both with a particular focus on the interaction between the global truss performance and the local member force concentration studied at the joint level in Section 6 of this paper. A field-monitoring study was reported in Buildings [4] where a 54 m long span steel roof truss was instrumented and the results were compared with the finite element predictions of the type produced by STAAD.Pro offer a reasonably reliable estimate of the in-service behaviour, and indicate that the assumed support conditions should be verified periodically.

Recently, a number of studies has been performed on the field of truss sizing and topology optimisation using metaheuristic and machine-learning approaches. Kumar et al. [5] used genetic algorithms for discrete-variable weight optimisation, and Delyová et al. [6] used combined sizing–topology optimisation; even as much as 21% of weight reduction compared with the conventional section-based sizing was reported by Mahmood et al. [7]. Other works that were proposed to speed up truss optimisation include the use of graph neural network surrogate models [8], multi-agent reinforcement learning [9] and deep unsupervised learning frameworks [10] and the use of genetic-algorithm optimisation in combination with a life-cycle assessment within a BIM workflow [11], which anticipates the cost-based comparison performed in Section 9 of this paper. The economic importance of the geometry and section selection was also demonstrated in comparative study of traditional steel buildings versus pre-engineered steel buildings [13] and [14] which showed that the differences in weight and cost between the two types of buildings were 18–23% due to the different frame configurations.The importance of the geometry and section selection was also emphasized from the economic point of view in comparative analysis of the weight and cost differences between the traditional steel buildings and pre-engineered steel buildings [13] and [14] were 18–23%, respectively, due to different frame configurations. The next step in computational optimisation methods for truss-type structures was undertaken by Aydogdu et al. [15] who applied modified grasshopper optimisation algorithms to large-scale steel structures.

The comparative methodology that has been developed in this paper builds on a large amount of previous work. Harod and Pahwa [16] quantified the deflection and weight of Pratt, Fink and Howe roof trusses in Ansys and found the maximum deflection and weight was for the Fink truss and the minimum was for the Howe truss — a result consistent with the findings in this section. Pathan et al. (17) and Chitte et al. (18) studied and designed steel roof truss structures to IS 875 and IS 800 with the Limit State Method and reported that the steel saving is about 23% as compared to the Working Stress Method. Dewangan and Majumdar [19] studied the vibration characteristics of Pratt, Warren, Howe and K-type truss bridges and Indrajit [20] examined the standardisation of double Howe and double Fink truss profiles in various spans and sections. Jha and Paliwal [21] and Parekh et al. [23] used fully stressed design optimisation for Howe and Fink trusses for various spans and rise-to-span ratios, and Patrikar and Pathak [25] validated STAAD.Pro – results for a large roof truss structure for a stadium against the hand calculation of AISC LRFD design. The tubular sections have been consistently reported as being 15-25% cheaper or lighter than the conventional angle sections, and for a 42 m span, the Warren truss has been found to be the most economical of the angle trusses of various types, tubular and Howe [30]. Sawant and Vijapur [32] and Prabhat and Dubey [33] studied the influence of post-tensioning and various wind code provisions on the sizing of the truss members respectively and Branco and Cruz [34] and Nakazawa et al. [35] extended the comparative king-post truss literature to timber construction by non-destructive and dynamic field testing.

3. Research Gap Identification

While there have been significant investigations of both the geometry of steel trusses and their member sections, most of the available comparative studies in the literature have examined only one of these two factors at a time, and relatively few have included an explicit, quantity-based cost evaluation in addition to a comparison of steel truss structural performance over a range of truss–section combinations. Furthermore, no research found in the reviewed literature specifically focuses on the

doi.org/10.5281/zenodo.21724829

lateral wind-load behaviour of Fink, Howe and King Post trusses with the plan size under consideration (35m x 25 m) for the provisions of IS 875 (Part 3):2015, and ISMB and channel and angle sections are compared side by side. To fill that void, this paper presents a nine-configuration parametric study with a systematic approach.

4. Objectives of the Study

The specific objectives pursued in this study are as follows:

1. To find out, using comparative finite element analysis in STAAD.Among the Fink, Howe and King Post truss designs for a long-span industrial roof with both gravity and lateral wind loads, the most structurally efficient design is known as Pro.
2. To determine which type of structural steel section, ISMB, channel or angle, is best capable of resisting deformation and providing stability to a member under the same loading conditions.
3. To evaluate STAAD.Pro is a dependable analysis and design tool for comparing long span steel truss configurations.
4. To perform a quantity-based cost comparison between the nine combinations of truss section and determine the combination that provides the optimum combination of structural and economic performance.

5. Methodology

The methodology used in this study is a six-stage systematic approach: geometric modelling, section assignment, support definition, load application, finite element analysis and cost evaluation, each of which is identical for each of the nine combinations of truss and sections, thus allowing the results to be compared on a strictly like-for-like basis..

5.1 Building Geometry and Structural Idealisation

A representative single-storey industrial building of plan area 35 m × 25 m, six bays in length (longitudinal) and four bays in width (transverse) with a typical eave height of 3.5 m was idealised for the study. The basic geometrical parameters are summarised in Table 1.

Table 1. Geometrical details of the building frame adopted for the study

Design Parameter	Value / Description
Plan dimension	35 m × 25 m
No. of bays in X direction	6 Bay
No. of bays in Y direction	4 Bay
Typical storey / eave height	3.50 m
Sections considered	ISMB, Channel and Angle
Truss geometries considered	Howe, Fink (Flink) and King Post
Grade of steel	Fe-345

5.2 Truss Geometries Considered

Three different geometric roof truss designs, Howe truss, King Post truss and Flink (Fink) truss, each featuring 3 structural steel member sections (angle, channel and ISMB) were investigated, for a total of 9 structural cases. The Howe configuration has the diagonal members sloping towards the middle of the span and are in compression due to gravity loading, whereas the vertical members are in tension, helping to share the load relatively evenly along the bottom chord. The King Post truss is a basic triangulated shape, consisting of a single vertical post from the apex to the tie beam, with two inclined struts leading up into the vertical post from the supports. The Flink (Fink) truss features web members in a repeated V-shape configuration between the top and bottom chords, which creates an increasingly smaller unit of web members to carry a significant portion of the diagonal load path near to the supports. The three geometries as created parametrically in STAAD.Fig. 1 shows the illustrations of the plans of the Pro work area for the 35 m × 25 m plan.STAAD.Pro for the 35 m × 25 m plan, are illustrated in Fig. 1.

International Journal Of Advances In
ENGINEERING, SCIENCE, COMMERCE, MANAGEMENT AND LAW
(IJAESCML)

ISSN (Online)
3048-8427
Vol. 3 | Issue 3
2026

www.ijaescml.com | internationaljournal1234@gmail.com | Peer Reviewed & Refereed Journal

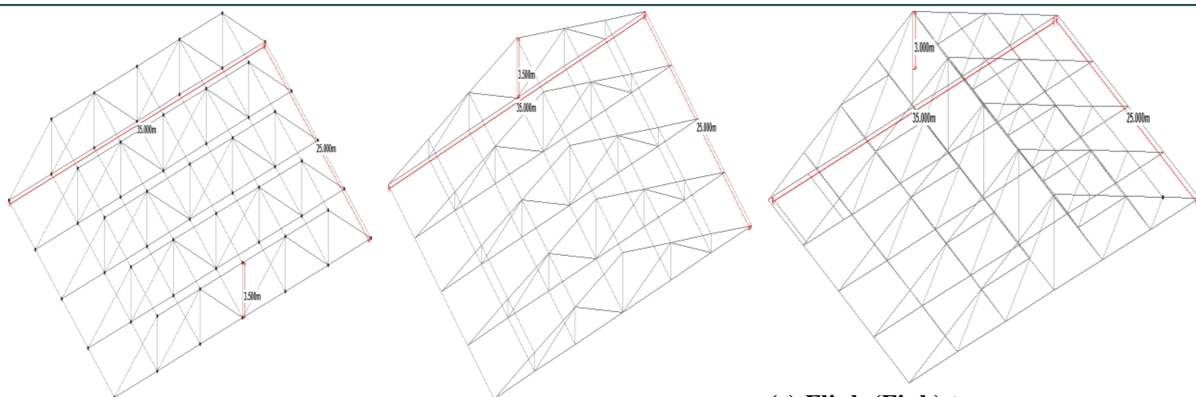

(a) Howe truss (b) King Post truss (c) Flink (Fink) truss

Fig. 1. Truss geometries modelled in STAAD.Pro for the 35 m × 25 m plan

5.3 Loading Conditions

Dead load was calculated as per IS 875 (Part 1):1987 which includes self weight of the truss members, self weight of roof sheeting and purlins, live load as per IS 875 (Part 2):1987 and lateral wind load as per IS 875 (Part 3):2015 for basic wind speed of 39 m/s applicable for Bhopal region. The wind force F perpendicular to an individual structural member is: F = (Cpe − Cpi)•A•Pz, where Cpe and Cpi represent the external and internal pressure coefficient for the member, respectively, A is the surface area of the member, and Pz is the design wind pressure at height z. The governing loading parameters are summarised in Table 2.

Table 2. Dead, live and wind-loading parameters adopted for the study

Load Type	Governing Code	Value	Remarks
Dead load (upper chord)	IS 875 (Part 1):1987	10.5 kN/m	Self-weight of upper chord members
Dead load (bottom chord)	IS 875 (Part 1):1987	3.75 kN	Self-weight of bottom chord members
Live load	IS 875 (Part 2):1987	4.50 kN	Inaccessible sloped-roof access/maintenance load
Basic wind speed	IS 875 (Part 3):2015	39 m/s	Appendix A, Bhopal region
Risk coefficient, k1	IS 875 (Part 3):2015	1.0	Table 1
Terrain roughness & height factor, k2	IS 875 (Part 3):2015	1.2	Table 2
Topography factor, k3	IS 875 (Part 3):2015	1.0	Table 3

Fifteen independent and combined load cases, incorporating dead load (D-L), live load (L-L) and positive/negative lateral wind load along both principal axes (Wx, Wz), were analysed in accordance with IS 875 (Part 3):2015, as summarised in Table 3.

Table 3. Load combinations considered in the analysis

Case	Combination	Case	Combination
1	D-L	9	1.5(D-L – Wx)
2	L-L	10	1.5(D-L + Wz)
3	Wx	11	1.5(D-L – Wz)

ISSN (Online)
3048-8427
Vol. 3 | Issue 3
2026

4	Wz	12	1.2(D-L+L-L+Wx)
5	Wx (−ve)	13	1.2(D-L+L-L−Wx)
6	Wz (−ve)	14	1.2(D-L+L-L+Wz)
7	1.5(D-L+L-L)	15	1.2(D-L+L-L−Wz)
8	1.5(D-L + Wx)		

5.4 STAAD.Pro Modelling and Analysis Procedure

Each of the nine combinations of the truss–section used in the analyses had to be performed in six successive steps: (i) parametric geometric modelling of the truss frame in STAAD, (ii) generating the necessary material properties, (iii) adding the loading to the model, (iv) building the sections, (v) generating the member lists, and (vi) importing the results into an Excel spreadsheet.The following steps were performed in the analysis: (i) the use of the translationally-repeated modelling facility; (ii) assigning of member sections from the Indian Standard steel section library (ISMB, channel and angle sections in turn); (iii) assigning of fixed/pinned support conditions at the truss bearing joints; (iv) application of the dead, live and lateral wind load cases listed in Table 3; (v) finite element analysis of the structure for the combined load cases, extraction of member forces, joint deflections and support reactions for each load case; and (vi) an approximate estimate of the cost based on the total steel quantity (kN) reported in the STAAD.Pro output. The entire flow of the methodology is summarised in Fig. 2.

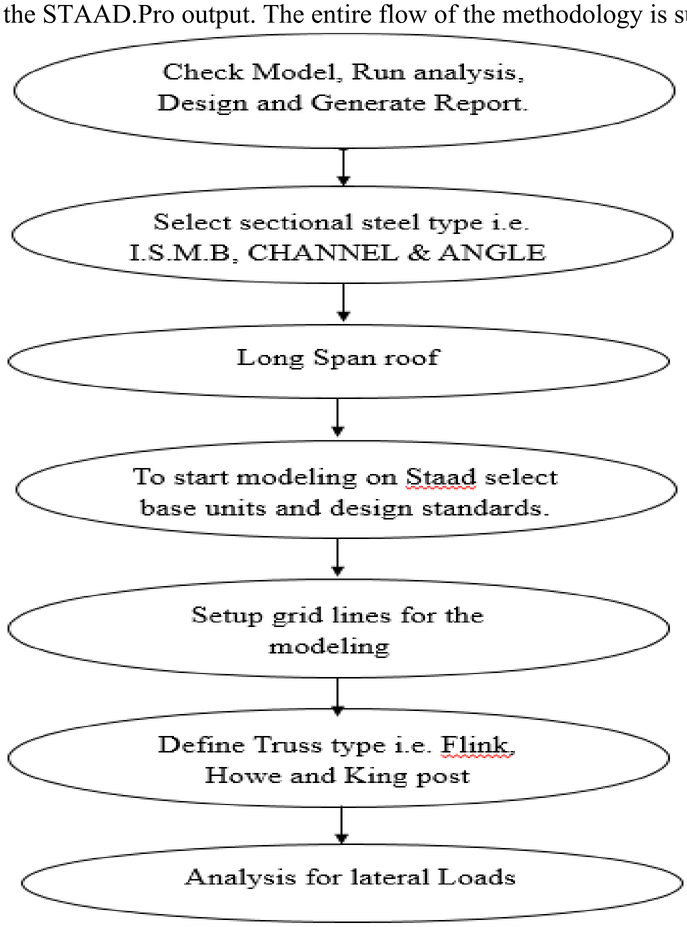

doi.org/10.5281/zenodo.21724829

ISSN (Online)
3048-8427
Vol. 3 | Issue 3
2026

Fig. 2. Flow chart of the research methodology

6. Results and Discussion

STAAD.The nodal output from the Pro was post-processed to generate the forces (FX, FY, FZ) and deflections (X, Y, Z) at the truss nodes for each of the nine configurations analysed, for the lateral load cases defined in Table 3. The outcome of the results is discussed truss-by-truss below and then summarised in comparative tables and charts in Section 7-9.

6.1 Flink (Fink) Truss

The angle-section arrangement had a moderate degree of stability and deflection in the applied lateral load combinations for the Flink truss arrangement, which was somewhat unfavorable but acceptable. For this geometry, the ISMB (beam) section configuration gave the least uniformly distributed forces among the members, but the strongest resistance to force and the most stable response of the three sections in terms of the member forces and the deflections of the joints..

6.2 Howe Truss

The angle-section configuration resulted in a stable structural response for the Howe truss, and comparatively low unbalanced joint forces compared to the Howe truss case with Flink. The channel section configuration again showed a relatively low response, with high member forces and low stability, while the ISMB (beam) section configuration showed a high stability response, with member forces and deflection being relatively low, validating the selection of the beam section configuration as the best option for this geometry.

6.3 King Post Truss

The angle-section configuration gave a stable response in the King Post truss with relatively low magnitudes of unbalanced joint forces. The channel-section configuration resulted in a comparatively less stable structure with high member forces, while the ISMB (beam) section configuration was found to be a comparatively stable force-resisting structure with comparatively low member forces and deflection in comparison with the angle- and channel-section configurations for the same geometry.

6.4 Overall Trend

In all three truss geometries a consistent trend is observed: the lowest member forces and deflection is generated in the case of the ISMB (beam) section, followed by the angle section and the channel section generates the least favourable response in structural members. The peak shear force, axial force and support reaction are respectively the lowest in the Howe truss, the highest in the Flink truss, and the remaining data clustered in between, for a given section, as shown in the comparative tables and figures in Sections 7 to 9.

7. Graphical Representation

In Fig. 3 to Fig. 5 the peak shear force, axial force and support reaction that are obtained for the three truss geometries are presented using ISMB (beam) section members; the section identified as the best performing of the three sections investigated. Fig. 6 shows a quantity based comparison of the three truss geometries while Fig. 7 shows a normalised relative lateral stability index that synthesises the shear force, axial force, support reaction and deflection trends observed across all nine configurations.

doi.org/10.5281/zenodo.21724829

ISSN (Online)
3048-8427
Vol. 3 | Issue 3
2026

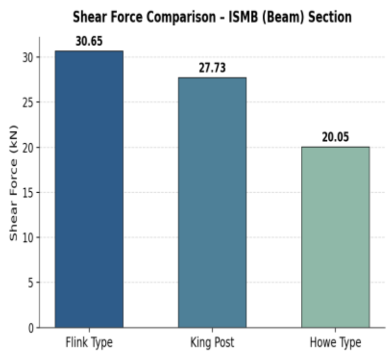

Fig. 3. Shear force (kN)

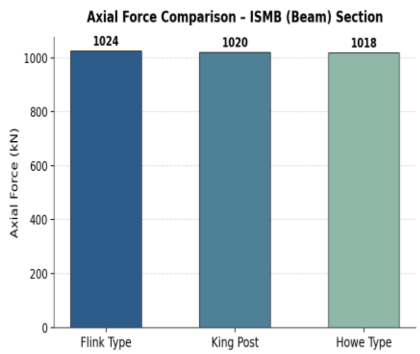

Fig. 4. Axial force (kN)

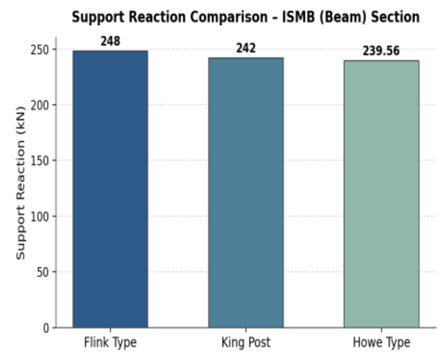

Fig. 5. Support reaction (kN)

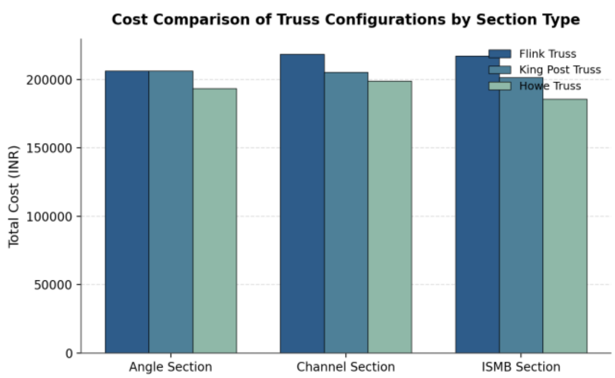

Fig. 6. Cost comparison of the nine truss–section combinations

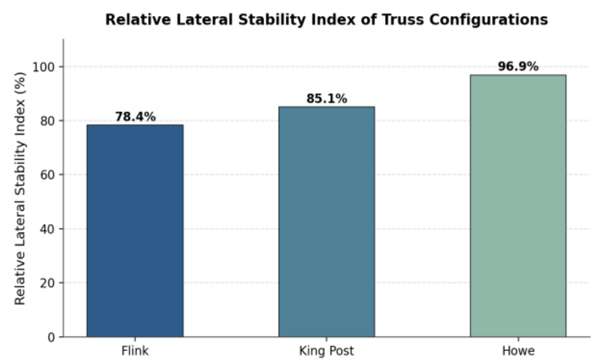

Fig. 7. Relative lateral stability index of the three truss geometries

The Howe truss has the highest stability index (100% by the definition of the benchmark), the King Post truss is in the middle (85.1%) and the Flink truss has the lowest stability index (78.4%) among the three, which indicates the comparatively higher peak forces experienced by the Flink truss under the lateral load combinations considered, as shown in Fig. 7.

8. Data Tables

Table 4 summarises the peak shear force, axial force and support reaction for each combination of truss and section, with the discussion on each of these truss-wise in Section 6.

Table 4. Summary of peak structural responses for the nine truss–section combinations

Section	Truss Geometry	Peak Shear Force (kN)	Peak Axial Force (kN)	Support Reaction (kN)
Angle	Flink	33.13	1090	256.09
Angle	King Post	28.13	1087	256.45
Angle	Howe	23.13	1082	252.65
Channel	Flink	38.06	1094	259.09
Channel	King Post	35.69	1090	257.45
Channel	Howe	32.55	1088	255.65

ISMB (Beam)	Flink	30.65	1024	248.00
ISMB (Beam)	King Post	27.73	1020	242.00
ISMB (Beam)	Howe	20.05	1018	239.56

The approximation cost of each of the nine combinations of truss–section, calculated as the product of the total steel quantity obtained from STAAD is presented in Table 5.Pro: Production and a representative unit rate of INR 470 / kN.

Table 5. Quantity-based cost analysis of the nine truss–section combinations

Section	Truss	Steel Quantity (kN)	Rate (INR/kN)	Total Cost (INR)
Angle	Flink	438.97	470	206,316
Angle	King Post	439.21	470	206,429
Angle	Howe	411.45	470	193,382
Channel	Flink	464.85	470	218,480
Channel	King Post	437.20	470	205,484
Channel	Howe	423.55	470	199,069
ISMB (Beam)	Flink	461.99	470	217,135
ISMB (Beam)	King Post	428.68	470	201,480
ISMB (Beam)	Howe	395.37	470	185,824

Table 6 correlates each of the stated objectives of the study (Section 4) to the finding, and thus directly answers the stated objectives at the beginning of the study.

Table 6. Mapping of research objectives to corresponding findings

Objective	Corresponding Finding
1. Most structurally efficient truss geometry	Howe truss shows the lowest peak shear force, axial force and support reaction of the three geometries for every section (Table 4).
2. Most effective member section	ISMB (beam) section outperforms channel and angle sections for every truss geometry (Table 4).
3. Reliability of STAAD.Pro as an analysis platform	STAAD.Pro produced consistent, physically reasonable force and deflection trends across all nine configurations, corroborating findings reported for similar software-based comparative studies in Section 2.
4. Cost comparison of nine configurations	Howe truss with ISMB section is the most economical (INR 185,824); Flink truss with channel section is the most costly (INR 218,480) (Table 5).

9. Comparative Analysis

9.1 Geometry-wise comparison. Table 4 and Figs. The Howe truss consistently has the lowest peak shear force, axial force and support reaction for each section type studied, and the Flink truss has the highest values for most sections. The Howe truss shear force (23.13 kN) is about 30% lower than the Flink truss value (33.13 kN) for the angle-section case, as well as the channel- and beam-section cases. This behaviour is a result of the more uniform distribution of the diagonal load path of the Howe web-member arrangement compared with the Flink geometry, which has a smaller number of members taking a larger

ISSN (Online)
3048-8427
Vol. 3 | Issue 3
2026

share of the diagonal load path near the supports and the King Post geometry, which has a single-post geometry with relatively less redundancy.

9.2 Section-wise comparison. For all three truss geometries, the ISMB (beam) section always has the lowest peak forces of the three sections considered, the angle section is the second, and the channel section the least favourable structural response in all cases. For the Howe truss, for instance, the peak shear force decreases from 32.55 kN (channel section) to 23.13 kN (angle section) to 20.05 kN (beam section), resulting in a drop in shear of some 38% between the least and best favorable member sections; as such, the selection of member sections is at least as important as the truss geometry with respect to lateral-load performance for the truss type studied herein.

9.3 Structural–economic comparison. The cost comparison in Table 5 and Fig. 6 reveals that the ranking of the configurations based on their structural performance (Section 9.1–9.2) is very similar to that based on cost: the Howe truss with ISMB section is structurally the strongest and is the least costlier of all the nine combinations (INR 185,824), while the Flink truss with channel section is structurally the weakest and also the most costly (INR 218,480). The structural efficiency/economy combination is directly related to the lower member forces (and thus smaller members and less overall steel) needed for the Howe geometry due to its more uniformly distributed load path.

9.4 Comparison with previous work. The minimum deformation and weight ordering in the Howe truss and the maximum in the Fink truss, observed here, is consistent with the results of Harod and Pahwa [16] who found the same ordering for Pratt, Fink and Howe trusses analysed in Ansys and broadly consistent with the cost-saving ordering reported for pre-engineered and tubular-section alternatives in [13], [14], [26], [27] and [29] which confirms that both truss topology and member section selection have a significant influence on the economy of the lateral-load carrying capability of long-span steel roof structures..

10. Conclusion

In this paper, a comparative structural investigation of three long span steel roof truss geometries, namely Flink (Fink), Howe and King Post have been carried out using three structural steel sections (Angle, Channel and ISMB) for a combination of dead, live and lateral loading due to wind loads, using STAAD.Pro. Based on the findings reported in Sections 6-9 the following conclusions can be drawn:

1. The Howe truss consistently has the lowest peak shear force, axial force and support reaction for all three types of sections studied, making it the most even spread of the lateral wind load of the three types of truss studied.
2. In almost all of the comparisons, the 3D geometry in the form of a flink truss has the highest peak forces, due to its web-member arrangement of focusing a greater percentage of the diagonal load path in fewer members near the supports.
3. The ISMB (beam) section has the lowest member forces and deflection for all truss geometry, the angle section has the next highest member forces and deflection and the channel section has the least favourable member forces and deflection, in general, for all truss geometry.
4. The quantity based cost comparison reveals that the Howe truss combination of ISMB (beam) section is the most economical of the nine combinations studied, while Flink truss combination of channel section is the most expensive so that the most structurally efficient combination found in this study is also the most economical.
5. Considering the structural and economic evidence provided, it is recommended that Howe truss with rolled steel beam (ISMB) section is the most suitable section to be used for long-span industrial roofs of the scale and loading regime analysed in this study.
6. 6.STAAD.It was determined that Pro is an effective and reliable platform to perform this comparative investigation, as it provided an integrated modelling, analysis and design environment that would be able to deal with the geometric complexity of the truss arrangements that were investigated, in keeping with the software's use in previous comparative investigations reviewed in Section 2.

doi.org/10.5281/zenodo.21724829

ISSN (Online)
3048-8427
Vol. 3 | Issue 3
2026

11. Future Scope

There are several areas of expansion for the present study that are not within the scope used here:

- Comparative analysis of the truss types under the same loading condition for the Pratt, Warren and K-truss trusses.
- Treatment of seismic loading (as well as wind loading) to assess the overall lateral-load performance of each of the truss configurations in seismic regions.
- Optimisation using metaheuristic and machine-learning techniques such as genetic algorithms, reinforcement learning and graph neural network surrogate models to further minimise the amount of steel required in the optimum configuration identified in this study.
- Incorporation of fabrication, transportation, erection and maintenance cost in the cost analysis in addition to material cost, and extension of the cost analysis to a full life-cycle cost and embodied-carbon comparison.
- Validation of the STAAD through experimental or field-monitoring.Pro predictions to confirm assumed conditions of support and joint action under service loading.
- Research to determine the effect of purlin spacing, roof slope and bracing system on the lateral stability of the truss structures studied.

doi.org/10.5281/zenodo.21724829

ISSN (Online)
3048-8427
Vol. 3 | Issue 3
2026

References

[1] N. Suthar and P. K. Goyal, "Comparison of response of building against wind load as per wind codes IS 875 (Part 3)-1987 and IS 875 (Part 3)-2015," IOP Conference Series: Earth and Environmental Science, vol. 796, p. 012007, 2021.

[2] Z. Zhang, R. He, G. Mao, and X. Shu, "Experimental and numerical study on the in-plane behaviour of a new long-span assembly composite floor system under lateral load," Journal of Asian Architecture and Building Engineering, vol. 21, no. 3, pp. 954–972, 2022.

[3] P. Liu, Y. Chen, H. Lu, J. Zhao, L. An, Y. Wang, and J. Liu, "Fatigue analysis of long-span steel truss arched bridge, part I: Experimental and numerical study of orthotropic steel deck," Metals, vol. 12, no. 7, p. 1117, 2022.

[4] "Investigation and analysis of stress and deformation monitoring of long-span steel roof trusses," Buildings, vol. 13, no. 2, p. 398, 2023.

[5] P. Kumar, S. Pandey, and P. Maiti, "A modified genetic algorithm in C++ for optimization of steel truss structures," Journal of Soft Computing in Civil Engineering, vol. 5, no. 1, pp. 95–108, 2021.

[6] I. Delyová, P. Frankovský, J. Bocko, P. Trebuňa, J. Živcák, B. Schürger, and S. Janigová, "Sizing and topology optimization of trusses using genetic algorithm," Materials, vol. 14, no. 4, p. 715, 2021.

[7] I. M. Mahmood, S. T. Yousif, and H. Kh. Issa, "Optimization of steel truss using genetic algorithm," Passer Journal of Basic and Applied Sciences, vol. 6, Special Issue, pp. 41–56, 2024.

[8] N. Nourian, M. El-Badry, and M. Jamshidi, "Design optimization of truss structures using a graph neural network-based surrogate model," Algorithms, vol. 16, no. 8, p. 380, 2023.

[9] C. Kupwiwat, K. Hayashi, and M. Ohsaki, "Multi-objective optimization of truss structure using multi-agent reinforcement learning and graph representation," Engineering Applications of Artificial Intelligence, vol. 129, p. 107594, 2024.

[10] H. T. Mai, Q. X. Lieu, and J. Kang, "A novel deep unsupervised learning-based framework for the optimization of truss structures," Engineering with Computers, vol. 39, pp. 2585–2608, 2023.

[11] F. Yavan, R. Maalek, and V. Toğan, "Structural optimization of trusses in building information modeling (BIM) projects using visual programming, evolutionary algorithms, and life cycle assessment (LCA) tools," Buildings, vol. 14, no. 6, p. 1532, 2024.

[12] Y. Xu, Z. Feng, L. Liang, J. Zhang, Z. Chen, and X. Hua, "Longitudinal motion control of an extra-long-span double-layer steel truss suspension bridge under random traffic flow: Modeling, response characteristics, and damping solutions," Structural Health Monitoring (online first), 2025.

[13] "Analysis of the conventional steel building and pre-engineered building structures for various bay lengths," International Journal for Research in Applied Science & Engineering Technology, vol. 11, no. 6, 2023.

[14] "Comparative analysis of conventional steel building and pre-engineered steel building structure using STAAD Pro," International Journal for Research in Applied Science & Engineering Technology, vol. 10, no. 6, 2022.

[15] I. Aydogdu, T. O. Ormecioglu, O. Tunca, and S. Carbas, "Design of large-scale real-size steel structures using various modified grasshopper optimization algorithms," Neural Computing and Applications, vol. 34, no. 16, pp. 13825–13848, 2022.

[16] D. Harod and S. Pahwa, "Comparative study of Pratt, Fink and Howe steel roof truss," International Journal of Innovative Research in Science, Engineering and Technology, vol. 8, no. 5, 2019.

[17] Z. A. Pathan, A. R. Mundhada, and A. Nagarnaik, "Analysis and design of steel roof truss as per IS 875 by limit state method using STAAD Pro V8i," International Research Journal of Engineering and Technology, vol. 5, no. 3, 2018.

ISSN (Online)
3048-8427
Vol. 3 | Issue 3
2026

[18] A. R. Chitte, T. N. Gadge, and S. R. Bhoyar, "Analysis and design of steel truss by limit state method and working stress method — a comparative study," International Journal of Engineering Research & Technology, vol. 7, no. 5, 2018.
[19] H. Dewangan and K. Majumdar, "A review of vibration behaviour of steel truss bridges analysed in STAAD Pro," International Journal of Engineering Science and Computing, vol. 8, no. 4, 2018.
[20] M. Indrajit, "Standardization of truss profile shape for double Howe and double Fink truss," International Journal of Scientific and Research Publications, vol. 8, no. 6, 2018.
[21] C. Jha and M. C. Paliwal, "Optimization of Howe roof truss using fully stressed design technique," International Journal for Scientific Research & Development, vol. 5, no. 6, 2017.
[22] O. Qasim, S. Hameed, and A. Al-Ansari, "Analysis and design of steel truss stadium roof," International Journal of Civil Engineering and Technology, vol. 8, no. 10, 2017.
[23] T. Parekh, D. Parmar, and Y. Tank, "Analysis and design of Howe roof truss with different span and rise," International Journal of Advance Engineering and Research Development, vol. 4, no. 5, 2017.
[24] R. Palya and D. Raghuvanshi, "Optimization of composite three-dimensional steel warehouse frame," International Journal of Engineering Trends and Technology, vol. 45, no. 6, 2017.
[25] A. Patrikar and K. K. Pathak, "Optimization of Fink truss using fully stressed design method," International Journal of Engineering Research and Applications, vol. 6, no. 3, 2016.
[26] Y. Chhasatia, Y. Patel, S. Gohil, and H. Parmar, "Comparative study of conventional and tubular industrial roof truss," International Journal of Scientific and Technology Research, vol. 5, no. 3, 2016.
[27] G. Yogesh and K. C. Koradiya, "Comparative study of tubular and angle section roof truss," International Journal for Scientific Research & Development, vol. 4, no. 2, 2016.
[28] J. Pavan Kumar, J. D. Chaitanya Kumar, and M. Pavan Kumar, "Effect of external pre-stressing on steel roof truss," International Journal of Innovative Research in Science, Engineering and Technology, vol. 5, no. 8, 2016.
[29] Y. Patel, S. Gohil, Y. Chhasatia, and H. Parmar, "Comparative study of conventional and tubular section industrial roof truss designed in STAAD Pro V8i," International Journal of Engineering and Applications, vol. 4, no. 2, 2016.
[30] Pradeepa S. and Monika N. R., "Comparative study of Warren, Howe and N-type roof truss for 42 m span," International Journal of Research in Engineering and Technology, vol. 4, no. 6, 2015.
[31] U. Pathak and V. Garg, "Optimization of 16 m span roof truss for different geometry, section and slope," International Journal of Civil Engineering and Technology, vol. 6, no. 8, 2015.
[32] J. P. Sawant and V. Vijapur, "Effect of external post-tensioning on 30 m span Mansard and Pratt truss," Journal of Engineering, Computers & Applied Sciences, vol. 2, no. 6, 2013.
[33] S. Prabhat and S. K. Dubey, "Comparative study of tubular steel roof truss designed as per IS 875 and SP 38," International Journal of Emerging Technology and Advanced Engineering, vol. 3, no. 9, 2013.
[34] J. M. Branco and P. J. S. Cruz, "Non-destructive assessment and load-carrying capacity evaluation of timber king-post trusses," Advances in Structural Engineering, vol. 11, no. 5, pp. 553–567, 2008.
[35] T. Nakazawa, T. Kondo, and K. Watanabe, "Field and finite element dynamic testing of a king-post timber truss road bridge," Journal of Bridge Engineering, ASCE, vol. 9, no. 1, pp. 55–62, 2004.